TISSUE ENGINEERING: Part A
Volume 21, Numbers 7 and 8, 2015

DOI: 10.1089/ten.tea.2014.0363

Nitric Oxide Stimulates Matrix Synthesis and Deposition by Adult Human Aortic Smooth Muscle Cells Within Three-Dimensional Cocultures

Phillip Simmers, MS,[1] Arsela Gishto, MS,[1] Narendra Vyavahare, PhD,[2] and Chandrasekhar R. Kothapalli, PhD[1]

Vascular diseases are characterized by the over-proliferation and migration of aortic smooth muscle cells (SMCs), and degradation of extracellular matrix (ECM) within the vessel wall, leading to compromise in cell–cell and cell–matrix signaling pathways. Tissue engineering approaches to regulate SMC over-proliferation and enhance healthy ECM synthesis showed promise, but resulted in low crosslinking efficiency. Here, we report the benefits of exogenous nitric oxide (NO) cues, delivered from S-Nitrosoglutathione (GSNO), to cell proliferation and matrix deposition by adult human aortic SMCs (HA-SMCs) within three-dimensional (3D) biomimetic cocultures. A coculture platform with two adjacent, permeable 3D culture chambers was developed to enable paracrine signaling between vascular cells. HA-SMCs were cultured in these chambers within collagen hydrogels, either alone or in the presence of human aortic endothelial cells (HA-ECs) cocultures, and exogenously supplemented with varying GSNO dosages (0–100 nM) for 21 days. Results showed that EC cocultures stimulated SMC proliferation within GSNO-free cultures. With increasing GSNO concentration, HA-SMC proliferation decreased in the presence or absence of EC cocultures, while HA-EC proliferation increased. GSNO (100 nM) significantly enhanced the protein amounts synthesized by HA-SMCs, in the presence or absence of EC cocultures, while lower dosages (1–10 nM) offered marginal benefits. Multi-fold increases in the synthesis and deposition of elastin, glycosaminoglycans, hyaluronic acid, and lysyl oxidase crosslinking enzyme (LOX) were noted at higher GSNO dosages, and coculturing with ECs significantly furthered these trends. Similar increases in TIMP-1 and MMP-9 levels were noted within cocultures with increasing GSNO dosages. Such increases in matrix synthesis correlated with NO-stimulated increases in endothelial nitric oxide synthase (eNOS) and inducible nitric oxide synthase (iNOS) expression within EC and SMC cultures, respectively. Results attest to the benefits of delivering NO cues to suppress SMC proliferation and promote robust ECM synthesis and deposition by adult human SMCs, with significant applications in tissue engineering, biomaterial scaffold development, and drug delivery.

Introduction

During development, a soluble monomer of elastin (tropoelastin) secreted by aortic smooth muscle cells (SMCs) coacervates with microfibrils (e.g., fibrillin) and lysyl oxidase enzyme (LOX) to form a highly crosslinked and stable elastin.[1] Elastin regulates the maintenance of tissue homeostasis, modulates the vascular cell–cell and cell–tissue signaling pathways, and helps withstand blood pressure exerted on the vessel walls.[2–4] Such highly stabilized and crosslinked elastin resists proteolysis and undergoes little turnover under physiologic conditions.[5] However, when vascular elastin is congenitally malformed, damaged by local injury, or degraded by acquired diseases, it severely compromises vessel integrity, disrupts cellular interactions, initiates inflammation, and weakens vessel wall.[6] Under such conditions, elastin gene expression is downregulated, and the mature elastin is degraded by inflammatory markers (cytokines, elastases, interleukins) into soluble peptides, which subsequently interrupts elastin-SMC signaling pathways.[7–10] Elastin disruption encourages SMC hyper-proliferation and medial thickening, leading to reduced arterial compliance, hypertension, and aneurysm.[11–13] Since vascular tissues inherently possess a minimal self-repair capability, a potential solution to stabilize and perhaps heal a diseased aorta is to restore homeostasis *in situ* via regeneration of structural and

[1]Department of Chemical and Biomedical Engineering, Cleveland State University, Cleveland, Ohio.
[2]Department of Bioengineering, Clemson University, Clemson, South Carolina.

functional mimics of native elastin. Failure to reinstate healthy elastin matrix and suppress inflammation could lead to heightened risk for atherosclerosis, aneurysm expansion, and eventual catastrophic rupture.

Currently, there are no clinically proven methods to preserve or restore elastin matrix within diseased aortae. Recent approaches to stimulate cellular elastin synthesis include (1) coaxing healthy adult cells in two-dimensional (2D) cultures to crosslink exogenous elastin precursors into insoluble proteins, (2) assembling elastomers from polypeptide precursors, (3) developing scaffolds that could provide signals that are critical for elastin synthesis, (4) delivering biomolecules (e.g., IGF-1, TGF-β, cyclic GMP) to stimulate tropoelastin mRNA expression and corresponding protein synthesis *in vitro*, (5) imparting mechanical stimuli *in vitro* to modulate cell alignment, tropoelastin synthesis, and matrix deposition by SMCs, and (6) exogenously delivering matrix molecules (e.g., hyaluronan fragments) to SMC cultures.[14–21] Despite their relative merits, these approaches (1) barely generate elastic fiber-associated proteins that are critical to healthy cell signaling, (2) do not demonstrate the feasibility of generating structural and functional mimics of native elastin in bulk, and (3) are yet to provide evidence for clinically sustainable delivery at the site of diseased aortic section *in vivo*. Furthermore, these studies were performed using either neonatal SMCs or dermal fibroblasts, typically derived from rodents, which inherently possess high elastogenic potential.[22,23] Such efforts were also limited by the incremental deterioration of tropoelastin mRNA expression in adult vascular cells and the unavailability of cellular cues that can upregulate tropoelastin synthesis and robust crosslinking into mature elastin matrices.[18,24–26] This suggests that alternative approaches are needed to restore crosslinked elastin matrices within elastin-deficient aortae while minimizing proteolytic enzyme activity.

Nitric oxide (NO) is a ubiquitous biologically important signaling molecule, an endothelium-dependent relaxing factor continuously produced by NO synthase in the vascular endothelium (endothelial nitric oxide synthase [eNOS]), and helps regulate vascular tone.[27,28] Under diseased conditions, endothelial dysfunction reduces NO release, which, in turn, activates SMC phenotype, stimulates release of enzymes, and degrades elastin matrix fibers, compromising SMC-elastin signaling homeostasis.[29–31] Localized NO delivery from photocrosslinked PEG-based hydrogels has been shown to inhibit neointima formation in a rat carotid balloon-injury model.[32,33] Other studies showed NO delivery to inhibit proliferation, stimulate tropoelastin and LOX mRNA expression and synthesis by chick aortic SMCs, in a dose-dependent manner, although the amounts and quality of matrix elastin were never quantified.[34] These studies attest to the possible role of NO donors in promoting elastin synthesis at transcriptional and translational levels, and inhibiting inflammatory activity. This raises the possibility that if physiological NO levels are restored within the vascular microenvironment under diseased conditions, (1) SMC activation, enzyme release, and matrix degradation could be inhibited, (2) elastin synthesis and crosslinked matrix formation could be upregulated, and (3) disease progression regressed to predisease levels.

In this study, the benefits of delivering NO cues to human aortic SMC (HA-SMC) proliferation, vascular extracellular matrix (ECM; elastin, glycosaminoglycans, hyaluronan) synthesis and deposition, proteases (MMPs-2,9) and their inhibitors (TIMP-1) release, matrix crosslinking enzyme (LOX) expression and activity, and NO synthase (eNOS, inducible nitric oxide synthase [iNOS]) expression in vascular cells were investigated. Specifically, the effect of various NO concentrations, delivered exogenously to HA-SMCs cultured within a three-dimensional (3D) coculture microenvironment, in the presence or absence of human aortic endothelial cells (HA-ECs) cocultures, was evaluated both qualitatively and quantitatively.

Materials and Methods

Coculture platform development

The microfluidic coculture system utilized in this study was created using photolithography and soft-lithography techniques as detailed earlier.[35] Briefly, the platform was designed in SolidWorks (SolidWorks Corp.) and the mold was developed at Stanford Microfluidics Foundry. Using this mold, microfluidic chips (Fig. 1A) were created by replica molding with polydimethylsiloxane (PDMS; Dow

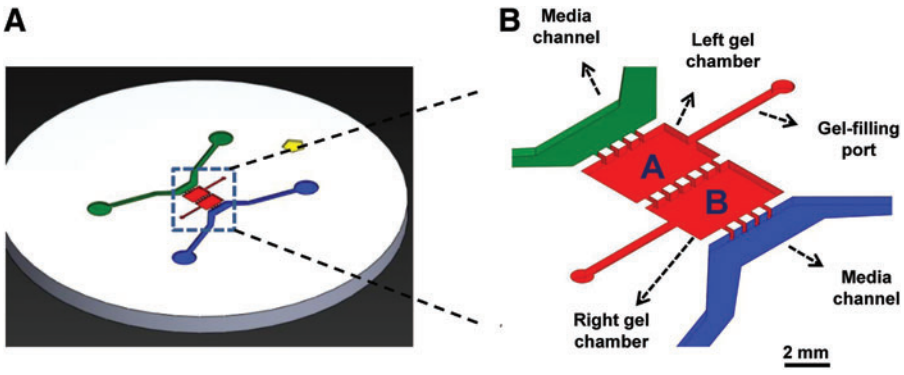

FIG. 1. **(A)** Design of the microfluidic device for enabling biomimetic cocultures. **(B)** Cells could be cultured either alone or in the presence of other cell types within designated chambers of the device. Cell chambers have individual gel-filling ports, separated by microfluidic pillar posts, and could be supplemented with media through separate channels (*blue* and *green shaded areas*). HA-SMCs were cultured within collagen scaffolds, in the presence or absence of endothelial cells (EC) coculture and exogenous GSNO (0–100 nM dosage). GSNO, S-Nitrosoglutathione; HA-SMCs, human aortic SMCs; SMCs, smooth muscle cells. Color images available online at www.liebertpub.com/tea

Corning). PDMS was mixed with curing agent (10:1 ratio), degassed and cured, removed from the mold, and cut into separate devices. The chips were then sterilized in boiling water (45 min) and dried (80°C, 2 h). The glass cover slips were cleaned with ethanol, air-plasma was treated along with PDMS devices for 60 s before bonding, and devices were stored till usage. Our long-term goal is to investigate the role of NO and cocultures under fluid flow conditions, and such a device would help us smoothly transition to this experimental setup. Transwell systems typically work better when both the cell types are cultured in 2D or in pseudo-3D.

Cell culture

Healthy adult human aortic smooth muscle cells (HA-SMCs) and HA-ECs were obtained from Life Technologies Corp. and passaged using appropriate media (Medium 231 and Medium 200, respectively; Life Technologies). For experiments in this study, we used cells from passages 3 to 5. A 500 μL collagen solution at 2 mg/mL concentration (pH ~7.4) was prepared by mixing type-1 collagen stock solution (111.85 μL; rat-tail derived, Corning®, 8.94 mg/mL master batch) with a mixture of 10× phosphate-buffered saline (pH ~7.4; 50 μL), 1 N NaOH (2.572 μL) and double-distilled water (335.57 μL), and maintained on ice till usage. Two sets of cultures were performed in parallel: (1) HA-SMCs cultured alone and (2) HA-SMCs cocultured with HA-ECs. Results from the former set serves to (i) establish baseline data for adult HA-SMC 3D cultures, (ii) act as a control for the adult vascular 3D coculture data, and (iii) rapidly scale up this process for further *in vitro* or *in vivo* studies. SMCs or ECs were mixed in 2 mg/mL collagen solution at a density of 10,000 cells per chamber. The coculture platform has two separate but adjacent 3D chambers (Fig. 1B), each with individual gel-loading ports and media channels. The chambers are separated from each other and from the media channels by 300×300 μm square posts (Supplementary Fig. S1A; Supplementary Data are available online at www.liebertpub.com/tea). These posts help in holding the gel within designated chambers due to surface tension. Each chamber is 2 mm in width (*x*-direction) between the posts, 3 mm in length (*y*-direction), and 150 μm in height (*z*-direction). Each chamber has a separate port for individual access, to enable flexibility in loading respective gels and cells, and also selectively remove gels postculture for biochemical analysis.

In devices where SMCs were cultured alone, collagen gel containing SMCs were injected in the right gel chamber of the device and collagen gel containing no cells in the left gel chamber. Similarly, in cases where cocultures were performed, collagen gel containing ECs were injected in the left gel chamber and gel containing SMCs in the right chamber. In this fashion, each cell type received its own media and S-Nitrosoglutathione (GSNO) dosage, yet in constant diffusive contact with neighboring cell type. Gels were injected into the respective gel-loading chambers with a cold-pipette tip containing ~7 μL of collagen solution. The devices were placed in a humidified incubator (37°C, 30 min) to polymerize collagen. On polymerization, cells were cultured for 21 days in either SMC or EC media (~250 μL in each media channel), containing GSNO (Sigma), as an NO donor.

Four different concentrations of GSNO (0, 1, 10, 100 nM) were tested for their ability to induce changes in SMC proliferation and matrix synthesis. We choose these concentrations because studies have shown that the physiological NO ranges from 10^{-4} to 10^{3} nM,[36,37] and in arteries it is within 0.1–500 nM.[38–41] GSNO at 0 nM concentration acts as a control for higher GSNO dosages in each case. Previous studies have shown that the half-life of GSNO ranges from 5.5 to 24 h, depending on pH and environmental conditions,[42,43] and is considerably higher than that of pure NO (typically a few minutes).[44] GSNO was shown to have a relatively high stability, decomposing with a rate constant of $0.018 \pm 0.002\ h^{-1}$ and a half-life of 38 ± 5 h.[43] At physiological concentrations, *S-N* bond of GSNO is enzymatically cleaved by thioredoxin system to liberate NO and a thiyl radical such as glutathione.[42] Such liberated low-molecular-weight thiols could, in turn, react with oxides of nitrogen to form S-nitrosothiols.[45] Therefore, we choose to replace the culture medium twice a day, so that fresh NO is delivered to the cells within cultures. The spent medium was pooled over the 21 day culture and stored at −20°C for further biochemical analyses. Similarly, cell matrix layers at the end of 21 days were trypsinized (one chamber at a time), pooled from respective chambers, and processed for biochemical assays as detailed next.

In general, contraction and shrinkage of collagen gels could be expected in long-term cultures, which might influence the biomechanical signaling experienced by the cells cultured within. In this study, we did not notice significant gel contraction within these devices over the 21 day culture (representative images shown in Supplementary Fig. S1B), possibly due to lack of external fluid shear across the gels, surface tension/adhesion between the gel and the upper and lower chamber surfaces, or fortification of collagen gels with new matrix deposition by cells. We choose not to coculture HA-SMCs with HA-SMCs (in separate chambers), due to minimum benefits from autocrine signaling. These devices could be scaled up in dimensions, for culturing larger gel volumes or higher cell densities. Although the concentrations of active ingredients within EC media (2% v/v fetal bovine serum, 10 ng/mL EGF, 10 ng/mL bFGF, 1 μg/mL hydrocortisone, 10 μg/mL heparin) are low, their effects, if any, would be normalized across the cases and therefore may not alter trends in data observed from these experiments.

DNA assay for cell proliferation

The cell density within different cases was quantified at the end of 21 days to assess the proliferation of HA-SMCs and HA-ECs over the culture period. Briefly, media was removed from the media channels ($n = 3$ devices/condition); 0.25% v/v trypsin-ethylenediamine tetraacetate (EDTA; Invitrogen) was added to the channels; cell layers were detached and extracted separately from each chamber, pelleted by centrifugation, resuspended in 1 mL of NaCl/Pi buffer (4 M NaCl, 50 mM Na_2HPO_4, 2 mM EDTA, and 0.02% Na-Azide; pH ~7.4), and sonicated for 3 min over ice; and a 100 μL aliquot was assayed using a fluorometric assay as detailed earlier.[46] The cell density was calculated on the basis of an estimated 6 pg DNA/cell.[47]

BCA assay for protein synthesis

The protein amounts synthesized by HA-SMCs under various culture conditions were determined using bicinchoninic acid protein assay kit (BCA Kit; Sigma-Aldrich), as

per the vendor's protocols. This assay is based on the principle that a Cu^{2+}-protein complex forms under alkaline conditions, followed by reduction of the Cu^{2+} to Cu^{1+} based on the amount of protein present in the sample. The protein in the pooled spent media as well as in the cell matrix at the end of 21 days was quantified ($n=6$ devices/condition). The total protein in pure 2 mg/mL collagen gels loaded within each designated chamber in the device was also quantified using this BCA assay. This amount was then excluded from the protein quantified within cell matrix under all the culture conditions, assuming that the collagen gel volume remained constant during the culture period. It should be noted that the protein amounts measured in pooled media will also contain the proteins from the 2% serum-additive media supplied to SMCs. This would not alter the statistical analysis of quantitative data, as such protein amounts are normalized across all the test cases in this study. The protein in pooled media and deposited as matrix also contain collagens synthesized and released by SMCs, which were not quantified in this study.

Fastin assay for elastin protein

The amounts of matrix elastin and tropoelastin (in pooled spent medium) were quantified using a Fastin assay (Accurate Scientific Corp), as previously detailed.[46] Since the Fastin assay quantifies only soluble α-elastin, the matrix elastin was first reduced to a soluble form by digesting with 0.25 N oxalic acid (1 h, 95°C) and filtering the pooled digestate in microcentrifuge tubes fitted with low-molecular-weight cut-off membranes (10 kDa). In parallel, aliquots of pooled spent medium over the 21 day culture were lyophilized and processed for tropoelastin using the Fastin assay ($n=6$ devices/condition). The measured amounts of matrix elastin and tropoelastin were normalized to their respective cell counts to provide a reliable basis of comparison between samples.

sGAG assay for glycosaminoglycan synthesis

The amounts of sulfated glycosaminoglycans (sGAGs) deposited within the cellular matrix as well as in the pooled spent medium were quantified using a quantitative dye-binding sGAG Assay (Kamiya Biomedical Company) as per vendor's protocols. This assay is based on the specific interactions between sulfated GAGs and the tetravalent cationic dye Alcian blue, at low pH and optimized ionic strength. It should be noted that this assay will not quantify the nonsulfated GAGs such as hyaluronic acid. The absorbance values were read at 620 nm on an Epoch™ microplate spectrophotometer (Bio-Tek), and the measured sGAG amounts were normalized to the corresponding cell counts ($n=6$ devices/condition). It should be noted that the sGAG amount measured in pooled media might also contain GAGs such as heparin (albeit in infinitesimal amounts) already present in the 2% serum-additive media supplied to SMCs.

HA assay for hyaluronic acid synthesis

Hyaluronic acid synthesized and released by SMCs within the cellular matrix as well as in the pooled spent medium was quantified using a hyaluronan enzyme-linked immunosorbent quantitative assay (Echelon Biosciences, Inc.). HA concentration in the sample is determined using a standard curve of known HA amounts. Absorbance values were read at 450 nm on an Epoch™ spectrophotometer, and the measured HA content was normalized to the corresponding cell counts ($n=6$ devices/condition).

LOX functional activity

Studies have shown that lysyl oxidase (LOX) and LOX-like proteins are endogenous enzymes responsible for crosslinking elastin precursor (tropoelastin) molecules. Thus, estimating the endogenous LOX activity in the cellular matrix indicates the extent of cell-mediated crosslinking of tropoelastin to form mature elastin matrix structures. Using a fluorometric assay (AmplexRed® Assay; Molecular Probes), we assayed for LOX activity within the cell matrix and pooled spent culture medium aliquots from different culture conditions. This assay works on the principle that H_2O_2 will be released when LOX oxidatively deaminates alkyl monoamines and diamines. Fluorescence intensities were recorded with excitation and emission wavelengths of 560 and 590 nm, respectively. The measured activity was normalized to the cell density within that respective culture condition ($n=3$ devices/condition). Although trypsinization of scaffolds to release cells and matrix proteins could affect LOX enzyme activity compared with that within spent pooled media, the effects are normalized across the samples and might not significantly alter the broad patterns observed here. Therefore, LOX enzyme activity within spent pooled media and within cell matrix were quantified, plotted, and discussed separately.

Western blot analysis for tropoelastin, LOX, eNOS, and iNOS

Western blot analysis was performed to semi-quantitatively confirm observed biochemical trends in tropoelastin synthesis and to assess LOX protein synthesis. In parallel, the expression of eNOS in EC cultures, and iNOS within SMC cultures (cultured alone, or in EC-cocultures), in the presence or absence of exogenous NO, was also semi-quantitatively assessed. As previously detailed,[46] samples of pooled spent medium were lyophilized and assayed for protein content using a DC protein assay kit (Bio-Rad Laboratories) to optimize loading sample amounts for SDS/PAGE Western blot. Protein bands were detected with respective primary polyclonal antibodies to elastin protein (Elastin Products), the 31-kDa active LOX protein (Santa Cruz Biotechnology), and the $\sim$135 kDa iNOS and eNOS proteins (both from Abcam). The bands were visualized by a chemiluminescence method according to vendor's specifications, and the images were quantified using NIH ImageJ.

Quantification of MMPs-2, 9 and TIMP-1 release

The amounts of MMPs-2 and 9 deposited within the cellular matrix as well as in the pooled spent medium were quantified using MMP-2 ELISA (Boster Biological Technology Co.) and MMP-9 ELISA (R&D Systems, Inc.) assays as per vendor's recommendations. The amount of TIMP-1 deposited within the cellular matrix as well as in the pooled medium was quantified using a TIMP-1 ELISA (Boster Biological Technology Co.). The measured MMPs

and TIMP-1 content were normalized to the respective cell count within those cultures ($n = 6$ devices/condition).

Immunofluorescence imaging of matrix proteins, iNOS, and eNOS

The presence of elastin, fibrillin, and LOX proteins within cell matrix was qualitatively confirmed using immunofluorescence labeling ($n = 3$ devices/condition for each protein). The presence of fibrillin within cell layers will confirm whether elastin matrix formation was mediated by predeposition of a fibrillin scaffold. Similarly, the expressions of iNOS and eNOS within SMC and EC cultures, respectively, were also assessed. At 21 days, the cell layers within microfluidic devices were fixed with 4% w/v paraformaldehyde for 15 min, and incubated with blocking serum (5% goat serum, 0.3% Triton-100 in phosphate-buffered saline; 20 min; 25°C). Elastin, fibrillin, and LOX were detected with respective polyclonal antibodies (Elastin Products; Abcam; Santa Cruz Biotechnology) and visualized with appropriate secondary antibodies (Chemicon), as detailed earlier.[46] Similarly, primary antibodies for iNOS and eNOS were obtained from Abcam to detect their expression. Cell nuclei were visualized with the nuclear stain 4′,6- diamino-2-phenylindole dihydrochloride (DAPI) contained in the mounting medium (Vectashield; Vector Labs). Images were acquired with a Zeiss Axiovert A1 florescence microscope equipped with Hamamatsu camera and image acquisition software.

Statistical analysis

All biochemical data were obtained from three independent repeat experiments per case and were analyzed using one-way analysis of variance followed by Tukey's HSD *post-hoc* testing, assuming unequal variance and differences deemed significant for $p < 0.05$. The data were assumed to follow a near-Gaussian distribution in all the cases, and the mean and standard errors were calculated accordingly.

Results and Discussion

Coculturing vascular cells within 3D scaffolds in close proximity to enable paracrine signaling has been reported by few groups. In efforts toward functionalizing 3D cardiovascular tissue engineering constructs, Pullens *et al.* evaluated the benefits of seeding a confluent human venous EC layer on myofibroblast-laden poly(glycolic acid) poly-4-hydroxybutyrate scaffolds, to collagen production by myofibroblasts.[48] Their results show that although the synthesis of collagen has been slightly reduced, mechanical properties of the constructs were significantly improved after coculturing with ECs for 1 week. Bulick *et al.* investigated the stand-alone and synergistic effects of rat EC coculture and mechanical conditioning on ECM production by rat SMCs within bilayered poly(ethylene glycol) diacrylate hydrogels.[49] They found that ECs and pulsatile flow synergistically increased elastin production and SMC differentiation, but suppressed collagen type I deposition. More recently, Bhattacharya *et al.* developed a coculture of human coronary artery cells in 3D poly(carbonate urethane) scaffolds to investigate EC-mediated Notch signaling and induction of SMC contractile phenotype.[50] These studies led to a critical understanding of the benefits of cocultures, mechanical stimuli, and 3D scaffolds to mimic physiological conditions, and investigated biological mechanisms under more controlled environments. Our current experimental setup differs from these previous studies as follows: (1) collagen gels were used in this study compared with synthetic polymeric scaffolds tested in previous studies; (2) human aortic ECs were cultured within 3D scaffolds in our study instead of a confluent monolayer, to enable paracrine signaling between ECs and SMCs; and (3) the microfluidic setup developed here would allow diffusion of paracrine signals and exogenous molecules under controlled static or dynamic flow conditions, depending on the experimental need.

The benefits of delivering NO from various types of biomaterials to promote healing and encourage matrix remodeling in vasculature have been gaining attention. Kim *et al.* recently demonstrated the benefits of encapsulating NO within liposomes and delivering in a rat subarachnoid hemorrhage model for treatment of vasospasm after subarachnoid hemorrhage.[51] Controlled release of NO from chitosan-based polymers has been shown to promote angiogenesis in diabetic mice with hind-limb ischemia and in the treatment of limb necrosis.[52] Naghavi *et al.* reviewed the recent progress made in the field of controlled NO release from various biomaterials for applications in cardiovascular therapy (e.g., thrombosis, intimal hyperplasia, device endothelialization).[53] Taken together, these studies attest to the numerous clinical applications of controlled delivery of exogenous NO from donors such as S-nitrosothiols.[54–56]

HA-EC and HA-SMC proliferation

The proliferation of HA-ECs and HA-SMCs cultured in the presence or absence of GSNO is shown in Figure 2. In the absence of GSNO (controls), ECs proliferated approximately three-fold over 21 days, compared with their original seeding density (Fig. 2A). The addition of 1 or 10 nM GSNO significantly promoted EC proliferation compared with day 1 seeding, although addition of 100 nM GSNO offered no benefit to EC proliferation compared with controls. In the presence or absence of GSNO, trends in SMC proliferation rates were different from those of ECs. When SMCs were cultured alone in the absence of ECs, increasing GSNO concentration suppressed SMC proliferation within 3D collagen scaffolds over the 21 day period (Fig. 2B). In the presence of EC cocultures, SMCs significantly proliferated at 0 and 1 nM GSNO concentrations. However, SMC proliferation rates significantly decreased at higher GSNO concentrations within cocultures.

We hypothesize that the NO release from GSNO concentrations tested here is within the physiological level,[44] which makes this study a good starting point for further *in vivo* optimization studies. Given that NO is an unstable gas and endogenous NO levels are tough to accurately quantify or manipulate, exogenous aerosolized NO delivery has been used to positively modulate circulating levels of NO within cystic fibrosis patients.[57] In this study, we did not investigate the NO activity and release rates from GSNO within culture media at neutral pH, as it has been extensively reported earlier.[45,58]

The molecular weight of NO is 30 Da and assuming it is spherical, the radius of NO molecule would be ~ 0.2 nm.[59] The diffusion coefficient of NO through a 2 mg/mL collagen

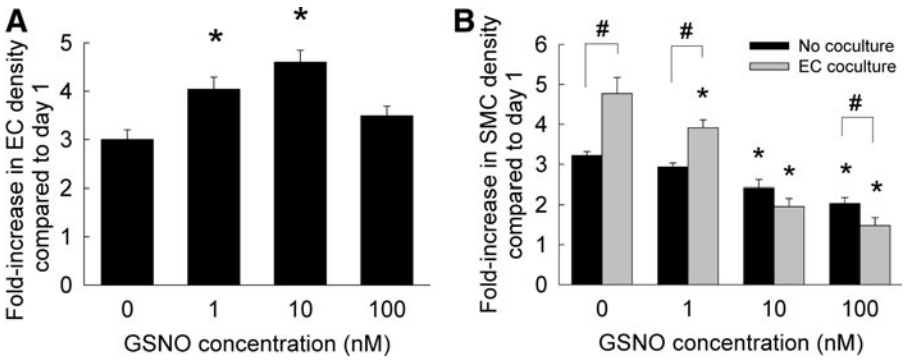

FIG. 2. **(A)** Fold increase in HA-EC density within 3D cultures supplemented with GSNO (0–100 nM). **(B)** Proliferation ratios of HA-SMCs in the presence or absence of EC cocultures and GSNO (0–100 nM). Data shown represent mean ± standard error of cell count after 21 days of culture, normalized to initial seeding density ($n = 3$/condition). $^{*}p < 0.01$ compared with GSNO-free cultures; $^{\#}p < 0.01$ for no cocultures versus EC coculture, at a given GSNO dosage. 3D, three-dimensional; HA-EC, human aortic endothelial cell.

scaffold was calculated using Stokes-Einstein equation, $D_c = kT/6\pi\eta R$, where k is Boltzmann constant (1.38065E-23 J/K), T is temperature (298.15 K), η is the viscosity of 2 mg/mL collagen gel (0.0104 kg/m·s; provided by vendor), and R is the Stokes radius (~ 0.2 nm). Thus, the diffusion coefficient (D_c) was calculated to be 1.0499E-12 m^2/s. Theoretically, the time it takes for a molecule to diffuse through a length L is given by, $\tau = L^2/4\pi^2 D_c$, where D_c is the diffusion coefficient. In our device, the length of collagen scaffold in the chamber is 2 mm, and so it takes ~ 965 s (i.e., 16 min) for the first NO molecule to reach the other end of the scaffold under non-convection conditions. Using these calculations, it takes ~ 32 min for a GSNO molecule (336 Da) to diffuse through 2 mg/mL collagen under similar conditions. However, in reality, diffusion times could be slightly different, taking into account the cells within the scaffold, molecular binding to scaffold, limited porosity arising from localized gel heterogeneity, and obstruction from newly deposited ECM. In conclusion, even in the absence of any induced flow, exogenously delivered NO diffuses rapidly from media channels through the 3D collagen scaffolds, to enable stimulation of SMCs and ECs within the scaffold.

Exogenously delivered NO has been shown to suppress proliferation of endothelial cells derived from fetal bovine aorta and human umbilical veins in a dose-dependent manner,[60] via an intracellular cGMP mechanism. In contrast, we noticed here that lower GSNO dosage (1–10 nM) promoted modest HA-EC proliferation, while the stimulatory effect was attenuated at 100 nM GSNO. Our results on the dose-dependent inhibitory effects of GSNO on HA-SMC proliferation are in excellent agreement with similar studies evaluating the role of NO donors (e.g., DETA NONOate, sodium nitroprusside, nitroglycerin, SNAP) on human, rabbit, chick, or rodent SMCs, both *in vitro* and *in vivo*.[34,44,58,61] Cell toxicity was not noted within our cultures (LIVE/DEAD assay, Supplementary Fig. S2) with the addition of GSNO, and cell morphology appeared identical in both controls and test cases. Thus, the suppression in SMC proliferation at higher GSNO dosages could be an outcome of intracellular downstream signaling pathways, the elucidation of which is beyond the scope of this work. SMC proliferation data within cocultures was also in agreement with studies by Fillinger *et al.*, who reported that within bovine aortic cell 2D cocultures, ECs stimulated SMC proliferation by $\sim 56\%$ compared with culturing SMCs alone.[62] Taken together, our results suggest that vascular cell proliferation is differentially modulated by exogenous NO delivery, with significant implications in vascular remodeling under healthy and diseased conditions.

Protein synthesis by HA-SMCs

The protein amounts synthesized by HA-SMCs, in the presence or absence of ECs, were quantified as two separate components; released into pooled spent media; and that was deposited within cell matrix. HA-SMCs produced and deposited $\sim 131 \pm 19$ ng of protein within cell matrices, on a per cell basis, when cultured alone in the absence of GSNO (Fig. 3A). Although 1 and 100 nM GSNO offered no further benefits to protein deposition within these SMC cultures, 10 nM GSNO significantly suppressed protein deposition within SMC cultures. On the other hand, coculturing SMCs with ECs did not improve protein deposition in cell matrix in the absence of GSNO. Within EC cocultures, only 100 nM GSNO stimulated an increase in protein deposition within cell layers, compared with GSNO-free cultures or lower GSNO doses. It should be noted that in these BCA assays, the amount of protein within SMCs was not separated from the total protein amount in the cell matrix.

HA-SMCs released $\sim 2 \pm 0.15$ μg of protein into pooled media on a per cell basis, over the 21 day culture, in the absence of EC cultures and GSNO (Fig. 3B). While the addition of 1 and 10 nM GSNO did not alter these amounts, 100 nM GSNO upregulated protein release. Surprisingly, coculturing with ECs significantly suppressed protein release into pooled media by SMCs, on a per cell basis, compared with their stand-alone cultures. Although addition of 1 nM GSNO did not rescue decrease in protein synthesis by SMCs within cocultures, 10 or 100 nM GSNO addition stimulated increases in protein synthesis compared with controls. Taken together, results suggest that 100 nM GSNO dosage significantly increased protein synthesis, release into pooled media, and deposition within cell matrix layers, in the presence or absence of EC cocultures.

The effects of NO on matrix protein synthesis by SMCs or any other mammalian cell types has been reported in a very few studies thus far. Kolpakov *et al.* have shown that NO donors such as SNAP (0.4–1.2 mM) and SNP (0.1–0.5 mM) inhibited total protein synthesis and collagen synthesis by rabbit aortic SMCs *in vitro* in a reversible but

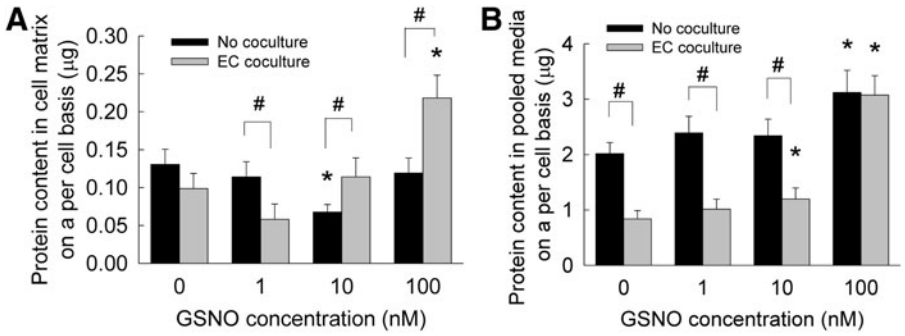

FIG. 3. Protein amounts deposited within cell matrix **(A)** or released into pooled media **(B)**, when GSNO (0–100 nM) was supplemented to HA-SMC cultures, in the presence or absence of HA-EC cocultures. Here, the protein amounts within SMCs was not separated from the overall protein quantified in the cell matrix (shown in **A**). Data shown represent mean ± standard error of protein synthesis after 21 days of culture, normalized to cell count within respective cases ($n = 6$/condition). $^{*}p < 0.05$ compared with GSNO-free cultures; $^{\#}p < 0.01$ for no cocultures versus EC coculture, at a given GSNO dosage.

dose-dependent manner,[63] highlighting the role of NO in modulating SMC phenotype. In another study, SNAP inhibited total protein synthesis by rat aortic SMCs in a time-dependent manner, when cultured in the presence of 5% fetal calf serum.[64] Curran *et al.* have shown that SNAP inhibited total protein synthesis by hepatocytes in a reversible but dose-dependent manner.[65] In this study, NO delivered from GSNO did not significantly enhance total protein synthesis by HA-SMCs, except within cultures receiving 100 nM dosage and EC cocultures. Although investigating the mechanisms by which NO mediates inhibition of protein synthesis by SMCs is beyond the scope of this work, previous studies suggest that multiple biochemical pathways might be involved in this process.[63]

Elastin synthesis and deposition by HA-SMCs

The total elastin synthesized by HA-SMCs was quantified as that released into pooled media (i.e., tropoelastin) and that deposited into the cell layers (i.e., matrix elastin). Within SMC cultures over the 21 days, the tropoelastin content on a per cell basis increased with the addition of GSNO compared with its absence (Fig. 4A). In the absence of EC cocultures, 10 nM GSNO appeared to stimulate higher tropoelastin synthesis and release by HA-SMCs compared with other GSNO dosages. Even in the absence of GSNO, coculturing with ECs stimulated significantly higher amounts of tropoelastin release by SMCs (Fig. 4A) compared with that within no coculture cases. Within cocultures, addition of 10 or 100 nM GSNO furthered tropoelastin synthesis compared with that seen in controls, although no such benefit to tropoelastin synthesis was noted at 1 nM GSNO dosage.

In the absence of EC cocultures, matrix elastin deposited within HA-SMC cultures was undetectable at 0 nM GSNO (Fig. 4B). However, with increasing GSNO dosage, matrix elastin amounts on a per cell basis increased in a linear fashion, with significant differences noted between incremental GSNO dosages. Taken together, results suggest that (1) although adult HA-SMCs produce quantifiable tropoelastin over the 21 day culture period, they do not deposit detectable amounts of matrix elastin, in the absence of GSNO; (2) coculturing with ECs significantly upregulated tropoelastin and matrix elastin by adult HA-SMCs, even in the absence of GSNO; (3) GSNO addition significantly enhanced both tropoelastin release and matrix elastin deposition by SMCs in a dose-dependent manner, in the presence or absence of EC cocultures; and (4) EC coculture and 100 nM GSNO synergistically contributed to multi-fold increases in tropo- and matrix elastin by adult HA-SMCs. Overall, these results suggest that the presence of NO and ECs not only promoted tropoelastin production by SMCs but also encouraged formation of crosslinked matrix elastin (with the help of endogenous LOX) to result in functional elastin, desirable from a tissue engineering standpoint.

Despite recent progress in the field of vascular tissue engineering, elastin synthesis and deposition by vascular SMCs within 3D constructs remain a formidable challenge.[18,66] This is partially due to the highly reduced ability of adult SMCs, at both transcription and translation levels, to synthesize, release, and deposit mature elastin. Thus, the overarching goal of cellular or tissue engineering approaches is to stimulate these adult SMCs, using an optimal combination of biochemical and biomechanical cues, to deposit mature and crosslinked elastin within blood vessels. In a series of studies, we have shown that exogenous cues such as hyaluronan oligomers, TGF-β1, IGF-1, and LOX induced increases in elastin synthesis within 2D cultures of adult rat aortic SMCs.[46,67–70] Recently, Lin *et al.* have shown that surface topography affects elastin gene expression and protein synthesis by adult human coronary artery SMCs.[71,72] Elastin gene expression and protein synthesis by these cells increased significantly when cultured within 3D porous polyurethane scaffolds compared with their 2D culture counterparts, and the addition of TGF-β1 to these cultures furthered these trends. Such increases in elastin expression by SMCs within these 3D scaffolds were facilitated by Ras-ERK1/2 signal transduction pathways. However, these cells were cultured only till 14 days, which is not sufficient for elastin matrix deposition and maturation within cell layers. Ramamurthi and coworkers recently showed that adult human and rat SMCs produced higher elastin protein within 3D collagen gels exposed to exogenous growth factors or cyclical stretching conditions.[73,74] These studies point to the overall superiority of 3D scaffolds over 2D cultures, in stimulating elastin synthesis and release by SMCs.

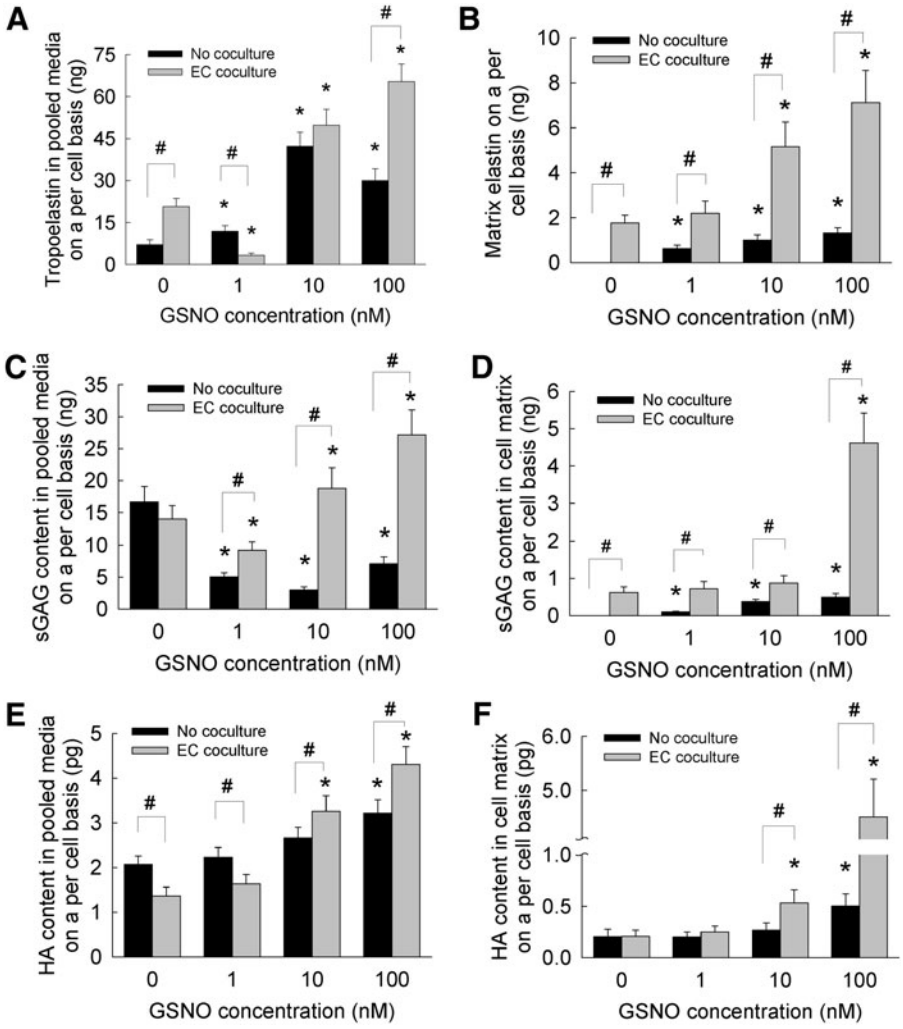

FIG. 4. Elastin protein released into pooled media **(A)** or deposited within cell matrix **(B)**, sulfated GAGs released into pooled media **(C)** or deposited within cell matrix **(D)**, and HA released into pooled media **(E)** or deposited within cell matrix **(F)**, when GSNO (0–100 nM) was supplemented to HA-SMC cultures, in the presence or absence of EC cocultures. Matrix elastin and tropoelastin were quantified using a Fastin® assay, sGAGs in pooled media and matrix quantified using a quantitative dye-biding sGAG Assay, and HA amounts in pooled media and matrix quantified using a hyaluronan enzyme-linked immunosorbent quantitative assay. Data shown represent mean ± standard error of protein synthesis after 21 days of culture, normalized to cell count within respective cases ($n = 6$/condition). $^{*}p < 0.05$ compared with GSNO-free cultures; $^{\#}p < 0.01$ for no cocultures versus EC coculture, at a given GSNO dosage.

Thus, in this study, we cultured HA-SMCs within 3D collagen scaffolds under coculture conditions, and enable future tissue engineering-based approaches for *in situ* elastin regeneration. We noted multi-fold increases in tropoelastin production and matrix elastin deposition within HA-SMC 3D cultures, in the presence of GSNO and EC cocultures. Interestingly, similar trends shown in Figure 4A and B were noted when the absolute amounts of tropoelastin and matrix elastin were normalized to the protein amounts quantified within pooled media and cell matrix (Fig. 3), respectively. A study by Sugitani *et al.* was the only known report that evaluated the role of NO on elastin expression and synthesis by chick aortic SMCs.[34] Although elastin deposition into matrix was not evaluated by them, results showed NO to stimulate tropoelastin mRNA expression, synthesis, and release into pooled media by chick cells in a dose-dependent manner (1–100 nM), with the maximum stimulation noted at 100 nM GSNO. Given that the adult human SMCs inherently do not produce much crosslinked elastin, increases in matrix elastin within GSNO and EC cocultures in the absence of external mechanical stimuli are quite relevant and encouraging from a tissue engineering and regenerative medicine standpoint. However, further studies are needed to quantify the changes in elastin gene expressions under these culture conditions, and provide a better explanation for the observed high matrix elastin content at specific GSNO dosages.

Glycosaminoglycan synthesis by HA-SMCs

Studies have shown that chondroitin sulfate and heparan sulfate were the main constituents of sGAGs produced by HA-SMCs.[75] Suarez *et al.* have shown that growth factors such as EGF, FGF, and VEGF stimulate SMCs to synthesize heparin sulfate in a dose-dependent manner.[76] However, the role of NO or EC cocultures in mediating GAG (sulfated or nonsulfated) synthesis remains unexplored, and this study reports for the first time the dose-dependent effects of NO donors on GAG synthesis by HA-SMCs. In general, the GAG content within the cell layers and pooled media was quantified as sulfated GAGs (sGAGs) and nonsulfated GAGs (HA). In the absence of EC cocultures, GSNO addition (1–100 nM) significantly suppressed sGAG release into pooled media when compared with controls (Fig. 4C). Although no further benefit of EC coculture to sGAG release into pooled media was noticed within GSNO-free cultures, presence of 1 nM GSNO suppressed sGAG release by SMCs, while 10 and 100 nM GSNO stimulated sGAG

release compared with controls ($p < 0.01$ for 1 nM vs. 10 nM or 100 nM; $p < 0.01$ for 10 nM vs. 100 nM GSNO). Taken together, except within GSNO-free cultures where significant differences were not noticed, coculturing with HA-ECs appeared to stimulate sGAG release by HA-SMCs in a GSNO dose-dependent manner.

The sGAG content deposited within cell matrices seems to reflect the trends observed in matrix elastin synthesis by HA-SMCs. sGAGs presence could not be detected within HA-SMC cell layers in the absence of EC coculture and GSNO (Fig. 4D). However, in the absence of EC cocultures, increasing GSNO concentration from 1 to 100 nM promoted significant sGAGs deposition in the cell layers in a dose-dependent manner ($p < 0.01$ for 1 nM vs. 10 nM or 100 nM; $p < 0.01$ for 10 nM vs. 100 nM). In the presence of EC cocultures, although 1 or 10 nM GSNO did not further promote sGAG deposition into matrix layers compared with that noted within GSNO-free cultures, 100 nM promoted a drastic increase in sGAG deposition within cell layers. Taken together, results show that 100 nM GSNO stimulated synthesis, release, and deposition of sGAGs by HA-SMCs within a 3D vascular coculture microenvironment. Interestingly, similar trends (Fig. 4C, D) were noted when the absolute amounts of sGAG content in pooled media and matrix were normalized to the protein amounts quantified within pooled media and cell matrix (Fig. 3), respectively.

The release of nonsulfated GAGs within SMC cultures was different from sGAG trends (Fig. 4E). In the absence of EC cocultures, no benefits to HA release were realized at lower GSNO dosages (0, 1 or 10 nM) except at 100 nM GSNO. However, in the presence of EC cocultures, GSNO at 0 and 1 nM suppressed HA release by SMCs into pooled media, although this suppression was rescued at higher GSNO dosages. The trends in HA deposition within cell matrix (Fig. 4F) mirrors those noted in sGAG deposition within respective cultures. When SMCs were cultured alone, only 100 nM GSNO stimulated an increase in HA deposition compared with lower GSNO dosages. Although no additional benefits of EC coculture were noted at 0 or 1 nM GSNO (Fig. 4F), a significant increase in HA deposition within cell layers was noted at 10 or 100 nM. Similar trends (Fig. 4E, F) were noted when the absolute amounts of HA content in pooled media and matrix were normalized to the protein amounts quantified within pooled media and cell matrix (Fig. 3), respectively.

Taken together, results show that 100 nM GSNO might help in the synthesis, release, and deposition of hyaluronic acid by HA-SMCs within vascular coculture environment. Our future studies are designed to elucidate the molecular weight ranges of hyaluronic acid fragments synthesized and released under respective conditions.

LOX enzyme activity

LOX has been shown to play an important role in the crosslinking and maintenance of ECM proteins such as elastin and collagen, and is, thus, expected to participate in ECM remodeling associated with cardiovascular diseases. However, LOX synthesis and activity within adult HA-SMC cultures has not been identified earlier. In this study, the LOX enzymatic activity was quantified within the cell matrix and pooled media to (1) establish the stand-alone and synergistic benefits of GSNO and EC cocultures to LOX activity, and (2) determine whether a correlation exists between LOX enzymatic activity and matrix protein amounts within respective cultures. In the absence of EC cocultures (Fig. 5A), LOX activity basal levels within pooled media drastically increased with the addition of 1, 10, and 100 nM GSNO. In GSNO-free cultures, EC coculture resulted in a 4.2-fold increase in LOX activity within pooled media, compared with that within SMC cultures. These levels were furthered with the addition of 1, 10, and 100 nM GSNO to SMC-EC cocultures.

The basal levels (0 nM GSNO) of LOX activity within cell matrix of SMC cultures increased significantly with the addition of 1, 10, and 100 nM GSNO (Fig. 5B). EC coculture provided no significant benefit to LOX activity within cell matrix, in the absence of GSNO. Surprisingly, 1 and 10 nM GSNO inhibited LOX activity within cell matrices in the presence of EC cocultures, while 100 nM GSNO promoted a dramatic 10.6-fold increase ($p < 0.001$ for 100 nM vs. lower dosages). This increase in LOX activity within cell matrix at 100 nM GSNO dosage, in the presence or absence of EC cocultures, partially explains the multi-fold increases in HA, elastin, and sGAG deposition within HA-SMC cell matrices. The only other known report on the effects of NO on LOX synthesis showed a 4.5-fold increase in LOX mRNA expression within chick aortic SMC cultures, with the addition of 100 nM GSNO.[34] We hypothesize that the increases in LOX activity seen at 100 nM GSNO and EC cocultures in our study might be due to a significant increase in LOX mRNA expression, which would be investigated in our future studies.

Western blot analysis semi-quantitatively confirmed the trends noted in tropoelastin synthesis and LOX activity within pooled media. Relative to GSNO-free controls, multi-fold increases in tropoelastin (Fig. 5C) and LOX protein (Fig. 5D) expression were noted within HA-SMC cultures with increasing GSNO concentration, and these increases were further enhanced in the presence of EC cocultures at higher GSNO dosages. Representative SDS-PAGE/Western blots containing bands corresponding to tropoelastin and LOX protein in pooled media are shown.

Release of MMPs-2, 9 and TIMP-1

The amounts of MMPs-2, 9 and TIMP-1 into pooled media were quantified on a per cell basis (Fig. 6). The amounts of these enzymes were insignificant to be accurately quantifiable in cell matrix. In the absence of EC cocultures (Fig. 6A), addition of 1–100 nM GSNO to SMC cultures suppressed MMP-2 release by 50–70% on a per cell basis. Coculturing with ECs suppressed MMP-2 release by SMCs, in the absence of GSNO. MMP-2 release within cocultures increased significantly within 10 or 100 nM GSNO cultures. On the other hand, MMP-9 levels increased marginally within SMC cultures in the presence of GSNO, compared with GSNO-free cultures (Fig. 6B). Within EC cocultures, MMP-9 levels were inhibited at lower GSNO concentrations (0–10 nM) compared with SMC cultures, although 100 nM GSNO increased MMP-9 release by SMCs for reasons not clear at this stage.

In the absence of cocultures (Fig. 6C), TIMP-1 levels were significantly suppressed by addition of 1 nM GSNO,

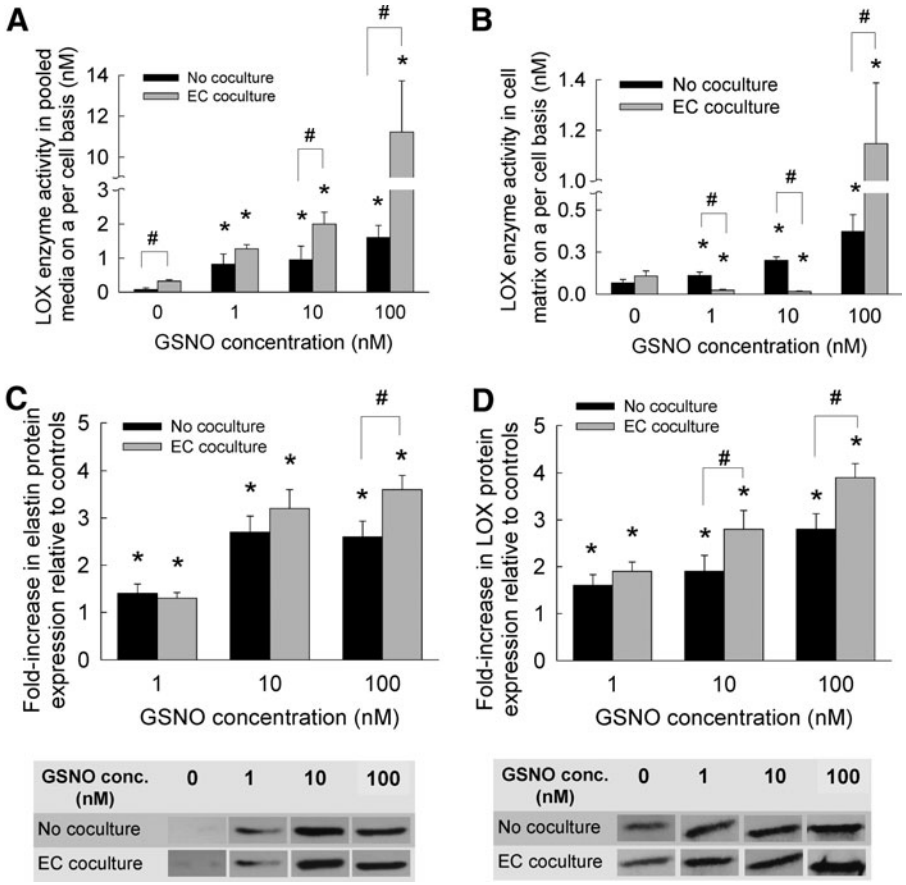

FIG. 5. LOX enzyme activity within pooled media **(A)** or within cell matrix **(B)**, when GSNO (0–100 nM) was supplemented to HA-SMC cultures, in the presence or absence of HA-EC cocultures. LOX activity was quantified using a fluorometric AmplexRed® assay. Data shown represent mean ± standard error of LOX synthesis after 21 days of culture, normalized to cell count within respective cases ($n = 6$ per condition). Data from western blot analysis showed fold increases in expression of elastin protein **(C)** and LOX protein **(D)** within pooled media, compared with GSNO-free cultures (controls). Representative SDS-PAGE/Western blots containing bands corresponding to tropoelastin and LOX protein in pooled media are shown for comparison. The protein bands were quantified in respective cases ($n = 3$ per condition) and normalized to controls. $^{*}p < 0.05$ compared with GSNO-free cultures; $^{\#}p < 0.01$ for no cocultures versus EC coculture, at a given GSNO dosage.

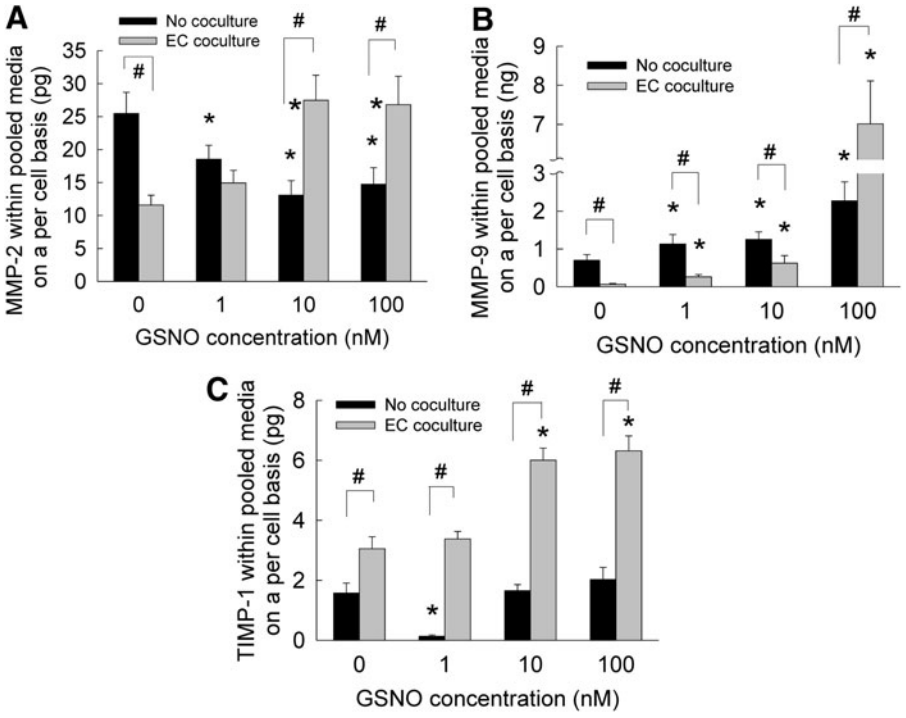

FIG. 6. The release of MMP-2 **(A)**, MMP-9 **(B)**, and TIMP-1 **(C)** into pooled media, when GSNO (0–100 nM) was supplemented to HA-SMC cultures, in the presence or absence of EC cocultures. Data shown represent mean ± standard error of protein synthesis after 21 days of culture, normalized to cell count within respective cases ($n = 3$ per condition). $^{*}p < 0.05$ compared with GSNO-free cultures; $^{\#}p < 0.01$ for no cocultures versus EC coculture, at a given GSNO dosage.

while 10 and 100 nM GSNO offered only marginal benefits compared with controls. Within EC cocultures, although 1 nM GSNO did not enhance basal levels of TIMP-1 release by SMCs, 10 and 100 nM GSNO promoted increases in TIMP-1 release into pooled media. In general, higher levels of TIMP-1 release were noted in cocultures compared with when SMCs were cultured alone. Taken together, these results suggest that (1) exogenous GSNO supplementation suppressed MMP-2 and marginally enhanced MMP-9 release when HA-SMCs were cultured alone, (2) MMP levels increased within cocultures with increasing GSNO, and (3) higher GSNO dosages enhanced the release of TIMP-1 by HA-SMCs in the presence of HA-EC cocultures.

Matrix metalloproteinases, specifically MMP-2 and MMP-9, play an important role in degrading basement membrane and ECM microenvironment, thus facilitating SMC migration during an injury or diseased (atherosclerosis, aneurysms, angioplasty, etc.) conditions in vasculature. On the other hand, naturally available tissue inhibitors of MMPs (e.g., TIMP-1) released by SMCs contribute to reduction in such ECM breakdown, SMC migration, and inflammation levels. Thus, a balance (or lack thereof) of these two components contributes to changes in SMC phenotype from quiescent to migratory and invasive nature. However, the specific levels of MMPs and TIMPs synthesized by adult human vascular SMCs within 3D cocultures are not known. Besides, very few studies explored the role of NO in regulating MMPs and TIMP levels within vasculature, under healthy or diseased conditions. In a recent study, Dey *et al.* reported on the molecular pathways involved in NO-mediated release of MMPs and TIMP by rat aortic SMCs *in vitro*.[77] They noted that in the presence of DETA NONOate, an NO donor, rat SMCs synthesized and secreted more MMP-2 and less amounts of MMP-9, while TIMP-2 levels increased as well. We hypothesize that the higher levels of MMPs and TIMP-1 noted within cocultures might be due to the combined release from SMCs and ECs, although further experiments are needed to quantify their release from ECs alone, and the effects of paracrine signaling between HA-ECs and SMCs.

Immunofluorescence labeling of elastin, fibrillin, and LOX

Immunofluorescence images under these culture conditions qualitatively support the elastin and LOX deposition within cell matrix layers discussed earlier. When SMCs were cultured alone within 3D scaffolds (Fig. 7), significantly higher staining for matrix elastin was noted within cultures supplemented with 10 and 100 nM GSNO, compared with that at 0 and 1 nM GSNO. Similar increases in LOX deposition were noted within cultures receiving higher dosages of GSNO. Although coculturing with HA-ECs resulted in higher amounts of matrix elastin deposition at all GSNO dosages, the staining intensity was more pronounced at higher GSNO concentrations (10 and 100 nM; Fig. 8). In agreement with quantitative data, a robust staining for LOX within 100 nM GSNO additive cultures was apparent, when SMCs were cocultured with ECs. Images from negative control cultures (stained without primary antibody) showed no coloration (data not shown). These data are in broad agreement with the quantitative data on matrix elastin (Fig. 4B) and LOX activity (Fig. 5B) within respective cultures. While staining for fibrillin expression could be seen within all the cases, it was modest and seems to be confined to the periphery of the cells. It also raises the possibility that adult HA-SMCs do not produce much fibrillin, although further studies are needed to precisely measure the ability of HA-SMCs to synthesize and deposit protein fibers (fibrillin, fibulins, MAGPs, etc.) that are important for elastin assembly and maturation. In general, staining for these proteins was evident in multiple focal planes within these 3D gels, contributing to diffuse staining and lack of clarity in images. Our current studies are elucidating the ultrastructure of the deposited elastin and matrix proteins (e.g., fibrillin co-localization) using a confocal microscope and a transmission electron microscope.

It could be seen that the combined amount of elastin and GAGs (quantified in Figs. 4 and 5), in both pooled media and cell matrix, is much lower than that quantified from BCA assay (Fig. 3). This suggests that in addition to elastin

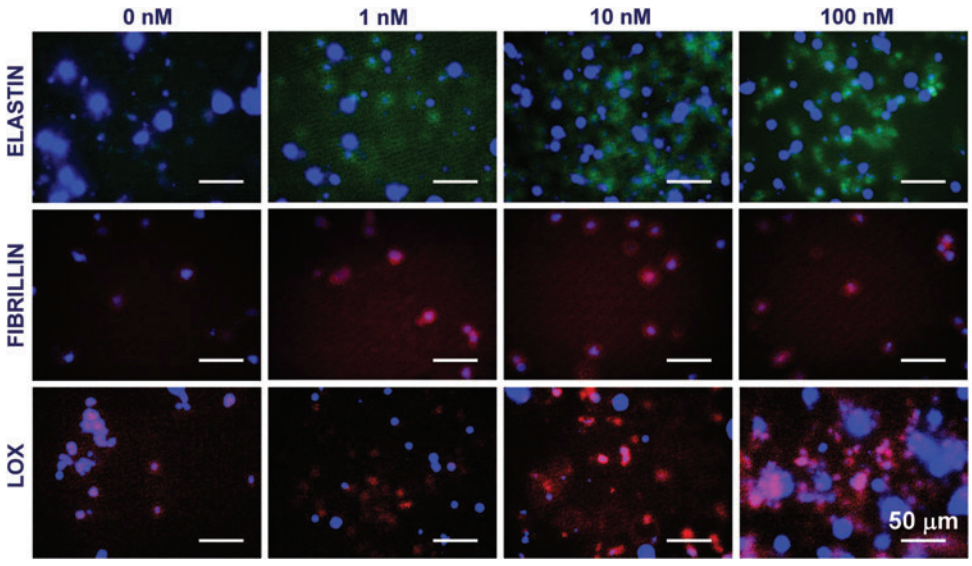

FIG. 7. Immunofluorescence images of elastin, fibrillin, and LOX proteins deposited by HA-SMCs within cell matrix layers, in the presence of GSNO (0–100 nM). HA-SMCs were cultured alone within 3D scaffolds, in the absence of cocultures with HA-ECs. Cultures were counter-stained with DAPI to visualize nuclei within these cell layers. Color images available online at www.liebertpub.com/tea

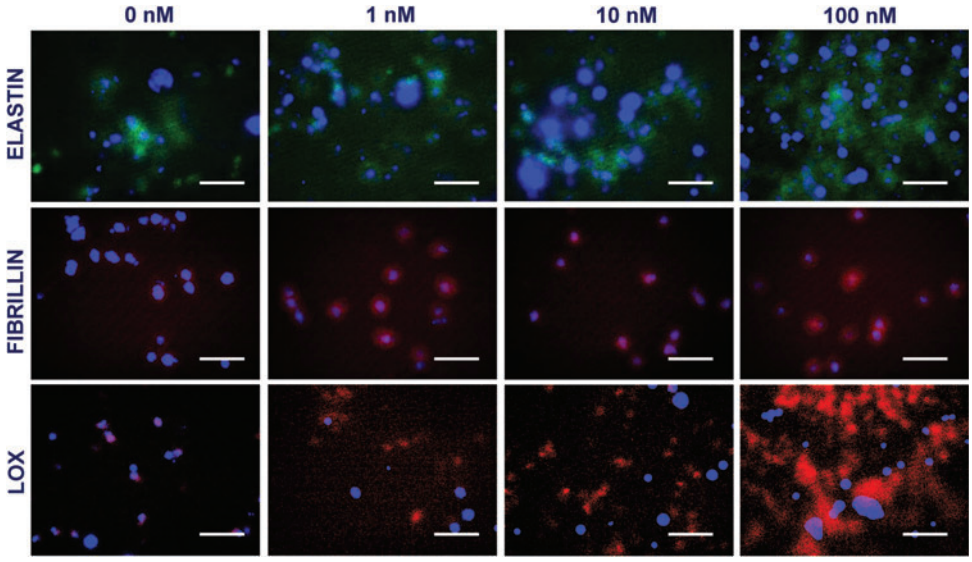

FIG. 8. Immunofluorescence images of elastin, fibrillin, and LOX proteins deposited by HA-SMCs within cell matrix layers, in the presence of GSNO (0–100 nM). HA-SMCs were cultured within 3D scaffolds, in the presence of cocultures with HA-ECs. Cultures were counterstained with DAPI to visualize nuclei within these cell layers. Scale bar = 50 μm. Color images available online at www.liebertpub.com/tea

and GAGs, numerous other proteins such as collagens and proteoglycans might be released and deposited by HA-SMCs within 3D scaffolds, which we intend to quantify in our future studies. Specifically, SMCs could be releasing collagens in response to external stimuli, and LOX enzyme promotes crosslinking and deposition of such collagens to further stiffen the matrix. However, since the SMCs were cultured within collagen scaffolds in this study, it is difficult to distinguish newly deposited collagen from existing 3D matrix scaffold, using conventional histology or biochemical assays. Our future studies will assess the changes in gene expression levels of various collagens in response to dose-dependent exogenous NO cues. Intuitively, we speculate that changing the composition or stiffness of the 3D scaffold might also influence the cell proliferation and matrix synthesis outcomes by HA-SMCs in the presence of GSNO. It is worth noting that the coculture setup presented here might not (1) represent the true interactions and paracrine signaling between ECs and SMCs *in vivo*, (2) mimic native EC-ECM interactions, or (3) reflect native effects of exogenous

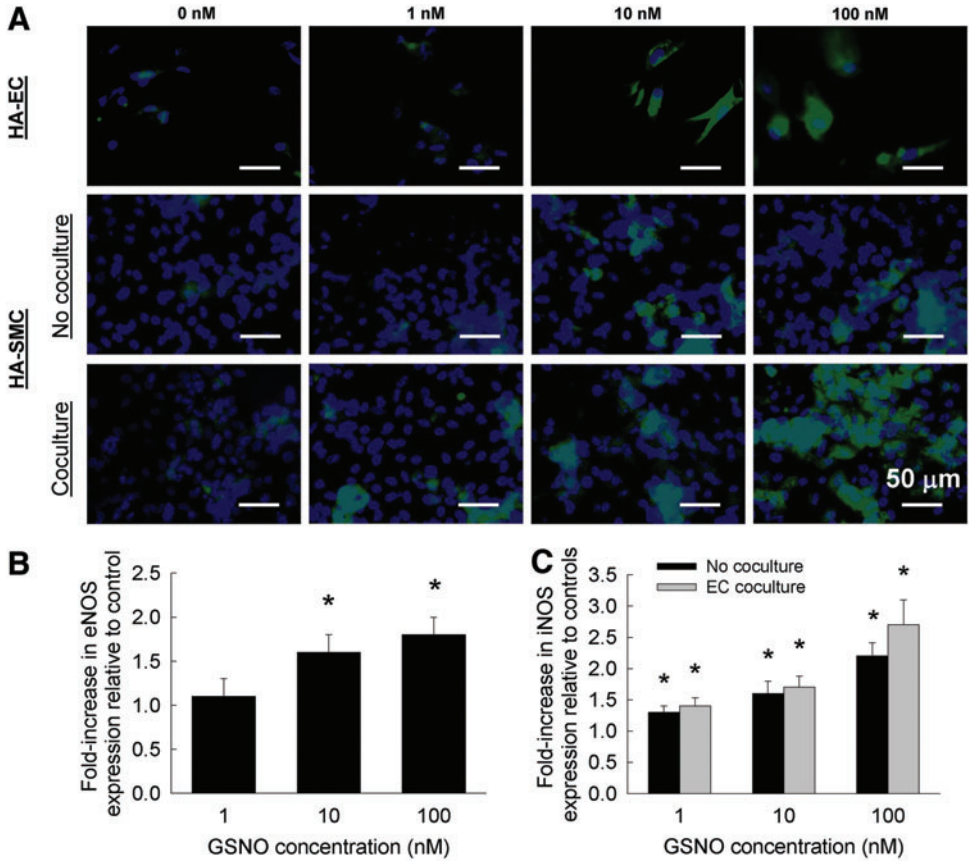

FIG. 9. **(A)** Immunofluorescence images of eNOS and iNOS expression within HA-EC and HA-SMC cultures, respectively, in the presence or absence of exogenous GSNO (0–100 nM). HA-SMCs were cultured either alone or cocultured with HA-ECs. From western blots of pooled media, eNOS **(B)** and iNOS **(C)** protein expressions were quantified and normalized to those noted within respective controls. eNOS, endothelial nitric oxide synthase; iNOS, inducible nitric oxide synthase. Color images available online at www.liebertpub.com/tea

NO delivery on vascular cells. It nevertheless serves as a good starting point to further refine the protocols involved in the development of a physiologically relevant *in vitro* culture setup, investigate vascular biology, and develop clinically applicable tissue engineering approaches.

iNOS and eNOS expression

Representative immunofluorescence images of eNOS expression within HA-EC cultures, in the presence or absence of exogenous NO, are shown in Figure 9A. Although faint eNOS expression could be noted within control cultures (0 nM NO), addition of 1 nM NO did not alter this expression. However, with 10 or 100 nM NO addition, a significant increase in eNOS staining could be noted. Results from Western blots on pooled media from these cultures support this qualitative data (Fig. 9B). A significant increase in eNOS protein expression was noted at 10 and 100 nM exogenous NO addition, compared with nonadditive controls. It is worth noting that no significant difference was noted in eNOS staining or protein expression between 10 and 100 nM NO additive cultures. Such GSNO-induced changes in eNOS expression were also reported by Kuo *et al.*, wherein intravenously injected GSNO (0.6 mg GSNO/kg) significantly increased plasma levels of NO and enhanced eNOS expression in a rat inferior epigastric artery flap.[78]

When HA-SMCs were cultured alone in the absence of EC cocultures, iNOS staining was very weak in both controls (0 nM) and at 1 nM GSNO exposure (Fig. 9A). However, iNOS staining significantly increased progressively with the addition of 10 and 100 nM GSNO within these cultures. Similar patterns of iNOS staining were noted within HA-SMC cultures, when cocultured with HA-ECs and supplemented with exogenous NO (Fig. 9A). Interestingly, coculturing with ECs seemed to promote iNOS staining with SMC cultures, and robust iNOS expression was noted within 100 nM NO additive SMC cultures. Western blots of iNOS protein expression within these cultures (Fig. 9C) suggested that (1) iNOS expression increased with increasing NO concentration within both no coculture and EC coculture conditions; and (2) no significant benefits of EC coculture to iNOS expression were realized at all NO concentrations. Taken together, these results suggest that exogenous NO supplementation was stimulating the endogenous expression of iNOS within HA-SMCs, and eNOS within HA-ECs, and coculturing these cells was compounding these benefits, resulting in significantly higher cell stimulation.

Although the physiological benefits of iNOS expression within diseased blood vessels remain controversial,[79–81] our results demonstrate a positive correlation between higher levels of iNOS expression and enhanced matrix synthesis, deposition, and LOX protein levels within HA-SMC cultures. Furthermore, such elevated levels of iNOS might enhance localized NO levels through its interaction with L-arginine, to further regulate the pathophysiology of blood vessels. Thus, our results also suggest that increasing iNOS expression within HA-SMCs, via exogenous delivery of NO donors, could help remodel matrix microenvironment under physiologically demanding conditions. Nevertheless, a systematic understanding of the complex pathways involved in NO-mediated SMC signaling is essential in formulating pharmaceutical approaches for the treatment of vascular degenerative diseases.

Conclusions

This study is based on the hypothesis that robust synthesis, organization, and maturation of elastin and GAGs within adult blood vessels could be accomplished, on demand, by exogenously delivering NO cues that proffer developmental signals and stimulate the intrinsic elastogenesis capability of adult HA-SMCs. Accordingly, a 3D cellular engineering approach has been developed and tested to evaluate the stand-alone and synergistic effects of NO and EC cocultures on the synthesis and deposition of matrix proteins on demand. Although the *in vitro* approach presented here may not be directly translational to an *in vivo* setting, it nevertheless establishes the baseline for NO dose that stimulates SMCs and promotes matrix deposition. We have observed that NO donor, such as GSNO, suppresses HA-SMC proliferation, encourages multi-fold increase in ECM protein (elastin, sGAGs and HA) synthesis and deposition, upregulates LOX release and enzymatic activity, and enhances TIMP-1 release within 3D collagen hydrogels, in a dose-dependent manner. Furthermore, it was noted that coculture with HA-ECs advances these patterns. Increasing GSNO concentration attenuated MMP-2 levels but not MMP-9 levels, and EC cocultures furthered these trends. This microfluidic platform and its variants could be extended to (1) coculture of other types of cells for elucidating paracrine signaling effects, (2) evaluate the effects of other physiologically relevant signaling molecules on ECM synthesis by SMCs, (3) test the role of fluid flow on cell behavior, and (4) investigate the role of ECM microenvironment on cell migration, proliferation, and matrix remodeling. Our current studies are geared to understand the signaling pathways involved in facilitating these NO-mediated trends on SMC behavior. Results from these studies not only serve as an experimental model for elucidating the role of NO in developmental stages of vasculature but also are highly relevant for drug and toxicology screening, tissue engineering and regenerative medicine therapies, and vascular disease remodeling.

Acknowledgments

The authors thank the Microfluidics Foundry at Stanford University for help with device molds and Mike Sawonik for help with the device design. The authors would also like to express their gratitude for the startup funds, Faculty Research Development Award (2012–2013), and Provost Undergraduate Research and Creative Achievement Award (2012) from the Cleveland State University. Partial support from NSF grant (1337859) to C.K. is also appreciated.

Disclosure Statement

No competing financial interests exist.

References

1. Li, D.Y., Brooke, B., Davis, E.C., Mecham, R.P., Sorensen, L.K., Boak, B.B., Eichwald, E., and Keating, M.T. Elastin is an essential determinant of arterial morphogenesis. Nature **393,** 276, 1998.

2. Robert, L., Jacob, M.P., and Fulop, T. Elastin in blood vessels. Ciba Found Symp **192,** 286, 1995.
3. Faury, G., Garnier, S., Weiss, A.S., Wallach, J., Fulop, T.J., Jacob, M.P., Mecham, R.P., Robert, L., and Verdetti, J. Action of tropoelastin and synthetic elastin sequences on vascular tone and on free Ca2+ level in human vascular endothelial cells. Circ Res **82,** 328, 1998.
4. Li, D.Y., Faury, G., Taylor, D.G., Davis, E.C., Boyle, W.A., Mecham, R.P., Stenzel, P., Boak, B., and Keating, M.T. Novel arterial pathology in mice and humans hemizygous for elastin. J Clin Invest **102,** 1783, 1998.
5. Fornieri, C., Quaglino, D.J., and Mori, G. Role of the extracellular matrix in age-related modifications of the rat aorta. Ultrastructural, morphometric, and enzymatic evaluations. Arterioscler Thromb **12,** 1008, 1992.
6. Ross, R. Cell biology of atherosclerosis. Annu Rev Physiol **57,** 791, 1995.
7. Rosenbloom, J., Abrams, W.R., and Mecham, R. Extracellular matrix 4: the elastic fiber. FASEB J **7,** 1208, 1993.
8. Galis, Z.S., and Khatri, J.J. Matrix metalloproteinases in vascular remodeling and atherogenesis: the good, the bad, and the ugly. Circ Res **90,** 251, 2002.
9. Mecham, R.P., Broekelmann, T.J., Fliszar, C.J., Shapiro, S.D., Welgus, H.G., and Senior, R.M. Elastin degradation by matrix metalloproteinases. Cleavage site specificity and mechanisms of elastolysis. J Biol Chem **272,** 18071, 1997.
10. Petersen, E., Gineitis, A., Wagberg, F., and Angquist, K.A. Activity of matrix metalloproteinase-2 and −9 in abdominal aortic aneurysms. Relation to size and rupture. Eur J Vasc Endovasc Surg **20,** 457, 2000.
11. Brooke, B.S., Bayes-Genis, A., and Li, D.Y. New insights into elastin and vascular disease. Trends Cardiovasc Med **13,** 176, 2003.
12. Keating, M.T. Elastin and vascular disease. Trends Cardiovasc Med **4,** 165, 1994.
13. Guo, D.C., Papke, C.L., He, R., and Milewicz, D.M. Pathogenesis of thoracic and abdominal aortic aneurysms. Ann N Y Acad Sci **1085,** 339, 2006.
14. Urry, D.W., Pattanaik, A., Xu, J., Woods, T.C., McPherson, D.T., and Parker, T.M. Elastic protein-based polymers in soft tissue augmentation and generation. J Biomater Sci Polym Ed **9,** 1015, 1998.
15. Bellingham, C.M., Lillie, M.A., Gosline, J.M., Wright, G.M., Starcher, B.C., Bailey, A.J., Woodhouse, K.A., and Keeley, F.W. Recombinant human elastin polypeptides self-assemble into biomaterials with elastin-like properties. Biopolymers **70,** 445, 2003.
16. Mithieux, S.M., Rasko, J.E., and Weiss, A.S. Synthetic elastin hydrogels derived from massive elastic assemblies of self-organized human protein monomers. Biomaterials **25,** 4921, 2004.
17. Lee, S.H., Kim, B.S., Kim, S.H., Choi, S.W., Jeong, S.I., Kwon, I.K., Kang, S.W., Nikolovski, J., Mooney, D.J., Han, Y.K., and Kim, Y.H. Elastic biodegradable poly(glycolide-co-caprolactone) scaffold for tissue engineering. J Biomed Mater Res A **66,** 29, 2003.
18. Bashur, C.A., Venkataraman, L., and Ramamurthi, A. Tissue engineering and regenerative strategies to replicate biocomplexity of vascular elastic matrix assembly. Tissue Eng Part B Rev **18,** 203, 2012.
19. Kim, B., Nikolovski, J., Bonadio, J., and Mooney, D.J. Cyclic mechanical strain regulates the development of engineered smooth muscle tissue. Nat Biotechnol **17,** 979, 1999.
20. Joddar, B., and Ramamurthi, A. Elastogenic effects of exogenous hyaluronan oligosaccharides on vascular smooth muscle cells. Biomaterials **27,** 5698, 2006.
21. Joddar, B., and Ramamurthi, A. Fragment size- and dose-specific effects of hyaluronan on matrix synthesis by vascular smooth muscle cells. Biomaterials **27,** 2994, 2006.
22. Fazio, M.J., Olsen, D.R., Kuivaniemi, H., Chu, M.L., Davidson, J.M., Rosenbloom, J., and Uitto, J. Isolation and characterization of human elastin cDNAs, and age-associated variation in elastin gene expression in cultured skin fibroblasts. Lab Invest **58,** 270, 1988.
23. Oakes, B.W., Batty, A.C., Handley, C.J., and Sandberg, L.B. The synthesis of elastin, collagen, and glycosaminoglycans by high density primary cultures of neonatal rat aortic smooth muscle. An ultrastructural and biochemical study. Eur J Cell Biol **27,** 34, 1982.
24. Johnson, D.J., Robson, P., Hew, Y., and Keeley, F.W. Decreased elastin synthesis in normal development and in long-term aortic organ and cell cultures is related to rapid and selective destabilization of mRNA for elastin. Circ Res **77,** 1107, 1995.
25. McMahon, M.P., Faris, B., Wolfe, B.L., Brown, K.E., Pratt, C.A., Toselli, P., and Franzblau, C. Aging effects on the elas-tin composition in the extracellular matrix of cultured rat aortic smooth muscle cells. In Vitro Cell Dev Biol **21,** 674, 1985.
26. Patel, A., Fine, B., Sandig, M., and Mequanint, K. Elastin biosynthesis: the missing link in tissue-engineered blood vessels. Cardiovasc Res **71,** 40, 2006.
27. Palmer, R.M., Ferrige, A.G., and Moncada, S. Nitric oxide release accounts for the biological activity of endothelium-derived relaxing factor. Nature **327,** 524, 1987.
28. Ignarro, L.J., Buga, G.M., Wood, K.S., Byrns, R.E., and Chaudhuri, G. Endothelium-derived relaxing factor produced and released from artery and vein is nitric oxide. Proc Natl Acad Sci U S A **84,** 9265, 1987.
29. Behr-Roussel, D. Cardiovascular risk factors, erection disorders and endothelium dysfunction. J Soc Biol **198,** 237, 2004.
30. Lüscher, T.F., and Noll, G. Endothelium dysfunction in the coronary circulation. J Cardiovasc Pharmacol **24,** S16, 1994.
31. Alonso, D., and Radomski, M.W. The nitric oxide-endothelin-1 connection. Heart Fail Rev **8,** 107, 2003.
32. Lipke, E.A., and West, J.L. Localized delivery of nitric oxide from hydrogels inhibits neointima formation in a rat carotid balloon injury model. Acta Biomater **1,** 597, 2005.
33. Masters, K.S., Lipke, E.A., Rice, E.E., Liel, M.S., Myler, H.A., Zygourakis, C., Tulis, D.A., and West, J.L. Nitric oxide-generating hydrogels inhibit neointima formation. J Biomater Sci Polym Ed **16,** 659, 2005.
34. Sugitani, H., Wachi, H., Tajima, S., and Seyama, Y. Nitric oxide stimulates elastin expression in chick aortic smooth muscle cells. Biol Pharm Bull **24,** 461, 2001.
35. Kothapalli, C.R., van Veen, E., de Valence, S., Chung, S., Zervantonakis, I.K., Gertler, F.B., and Kamm, R.D. A high-throughput microfluidic assay to study neurite response to growth factor gradients. Lab Chip **11,** 497, 2011.
36. Ahern, G.P., Hsu, S.F., and Jackson, M.B. Direct actions of nitric oxide on rat neurohypophysial K+ channels. J Physiol **520,** 165, 1999.
37. Ricciardolo, F.L., Vergnani, L., Wiegand, S., Ricci, F., Manzoli, N., Fischer, A., Amadesi, S., Fellin, R., and Geppetti, P. Detection of nitric oxide release induced by bradykinin in guinea pig trachea and main bronchi using a

porphyrinic microsensor. Am J Respir Cell Mol Biol **22,** 97, 2000.
38. Chen, K., and Popel, A.S. Theoretical analysis of biochemical pathways of nitric oxide release from vascular endothelial cells. Free Radic Biol Med **41,** 668, 2006.
39. Hall, C.N., and Garthwaite, J. What is the real physiological NO concentration in vivo? Nitric Oxide **21,** 92, 2009.
40. Mochizuki, S., Miyasaka, T., Goto, M., Ogasawara, Y., Yada, T., Akiyama, M., Neishi, Y., *et al.* Measurement of acetylcholine-induced endothelium-derived nitric oxide in aorta using a newly developed catheter-type nitric oxide sensor. Biochem Biophys Res Commun **306,** 505, 2003.
41. Tsoukias, N.M. Nitric oxide bioavailability in the microcirculation: insights from mathematical models. Microcirculation **15,** 813, 2008.
42. Nikitovic, D., and Holmgren, A. S-nitrosoglutathione is cleaved by thethioredoxin system with liberation of glutathione and redox regulating nitric oxide. J Biol Chem **271,** 19180, 1996.
43. Mancuso, C., Bonsignore, A., Di Stasio, E., Mordente, A., and Motterlini, R. Bilirubin and S-nitrosothiols interaction: evidence for a possible role of bilirubin as a scavenger of nitric oxide. Biochem Pharmacol **66,** 2355, 2003.
44. Isenberg, J.S., Wink, D.A., and Roberts, D.D. Thrombospondin-1 antagonizes nitric oxide-stimulated vascular smooth muscle cell responses. Cardiovasc Res **71,** 785, 2006.
45. Singh, S.P., Wishnok, J.S., Keshive, M., Deen, W.M., and Tannenbaum, S.R. The chemistry of the S-nitrosoglutathione/glutathione system. Proc Natl Acad Sci U S A **93,** 14428, 1996.
46. Kothapalli, C.R., Taylor, P.M., Smolenski, R.T., Yacoub, M.H., and Ramamurthi, A. Transforming growth factor beta 1 and hyaluronan oligomers synergistically enhance elastin matrix regeneration by vascular smooth muscle cells. Tissue Eng Part A **15,** 501, 2009.
47. Labarca, C., and Paigen, K. A simple, rapid, and sensitive DNA assay. Anal Biochem **102,** 344, 1980.
48. Pullens, R.A., Stekelenburg, M., Baaijens, F.P., and Post, M.J. The influence of endothelial cells on the ECM composition of 3D engineered cardiovascular constructs. J Tissue Eng Regen Med **3,** 11, 2009.
49. Bulick, A.S., Muñoz-Pinto, D.J., Qu, X., Mani, M., Cristancho, D., Urban, M., and Hahn, M.S. Impact of endothelial cells and mechanical conditioning on smooth muscle cell extracellular matrix production and differentiation. Tissue Eng Part A **15,** 815, 2009.
50. Bhattacharyya, A., Lin, S., Sandig, M., and Mequanint, K. Regulation of vascular smooth muscle cell phenotype in three-dimensional coculture system by JAGGED1-selective notch3 signaling. Tissue Eng Part A **20,** 1175, 2014.
51. Kim, H., Britton, G.L., Peng, T., Holland, C.K., McPherson, D.D., and Huang, S.L. Nitric oxide-loaded echogenic liposomes for treatment of vasospasm following subarachnoid hemorrhage. Int J Nanomedicine **9,** 155, 2014.
52. Zhao, Q., Zhang, J., Song, L., Ji, Q., Yao, Y., Cui, Y., Shen, J., Wang, P.G., and Kong, D. Polysaccharide-based biomaterials with on-demand nitric oxide releasing property regulated by enzyme catalysis. Biomaterials **34,** 8450, 2013.
53. Naghavi, N., de Mel, A., Alavijeh, O.S., Cousins, B.G., and Seifalian, A.M. Nitric oxide donors for cardiovascular implant applications. Small **9,** 22, 2013.
54. Kushwaha, M., Anderson, J.M., Bosworth, C.A., Andukuri, A., Minor, W.P., Lancaster, J.R., Anderson, P.G., Brott, B.C., and Jun, H.W. A nitric oxide releasing, self assembled peptide amphiphile matrix that mimics native endothelium for coating implantable cardiovascular devices. Biomaterials **31,** 1502, 2010.
55. Zhao, H., Serrano, M.C., Popowich, D.A., Kibbe, M.R., and Ameer, G.A. Biodegradable nitric oxide-releasing poly(diol citrate) elastomers. J Biomed Mater Res A **93,** 356, 2010.
56. Carpenter, A.W., and Schoenfisch, M.H. Nitric oxide release: part II. Therapeutic applications. Chem Soc Rev **41,** 3742, 2012.
57. Snyder, A.H., McPherson, M.E., Hunt, J.F., Johnson, M., Stamler, J.S., and Gaston, B. Acute effects of aerosolized S-nitrosoglutathione in cystic fibrosis. Am J Respir Crit Care Med **165,** 922, 2002.
58. Yu, H., Payne, T.J., and Mohanty, D.K. Effects of slow, sustained, and rate-tunable nitric oxide donors on human aortic smooth muscle cells proliferation. Chem Biol Drug Des **78,** 527, 2011.
59. Erickson, H.P. Size and shape of protein molecules at the nanometer level determined by sedimentation, gel filtration, and electron microscopy. Biol Proced Online **11,** 32, 2009.
60. Yang, W., Ando, J., Korenaga, R., Toyo-oka, T., and Kamiya, A. Exogenous nitric oxide inhibits proliferation of cultured vascular endothelial cells. Biochem Biophys Res Commun **203,** 1160, 1994.
61. Jeremy, J.Y., Rowe, D., Emsley, A.M., and Newby, A.C. Nitric oxide and the proliferation of vascular smooth muscle cells. Cardiovasc Res **43,** 580, 1999.
62. Fillinger, M.F., O'Connor, S.E., Wagner, R.J., Cronenwett, J.L., and Kent, K.C. The effect of endothelial cell coculture on smooth muscle cell proliferation. J Vasc Surg **17,** 1058, 1993.
63. Kolpakov, V., Gordon, D., and Kulik, T.J. Nitric oxide-generating compounds inhibit total protein and collagen synthesis in cultured vascular smooth muscle cells. Circ Res **76,** 305, 1995.
64. Garg, U.C., and Hassid, A. Mechanisms of nitrososthiol-induced antimitogenesis in aortic smooth muscle cells. Eur J Pharmacol **237,** 243, 1993.
65. Curran, R.D., Ferrari, F.K., Kispert, P.H., Stadler, J., Stuehr, D.J., Simmons, R.L., and Billiar, T.R. Nitric oxide and nitric oxide-generating compounds inhibit hepatocyte protein synthesis. FASEB J **5,** 2085, 1991.
66. Sivaraman, B., Bashur, C.A., and Ramamurthi, A. Advances in biomimetic regeneration of elastic matrix structures. Drug Deliv Transl Res **2,** 323, 2012.
67. Kothapalli, C.R., and Ramamurthi, A. Benefits of concurrent delivery of hyaluronan and IGF-1 cues to regeneration of crosslinked elastin matrices by adult rat vascular cells. J Tissue Eng Regen Med **2,** 106, 2008.
68. Kothapalli, C.R., and Ramamurthi, A. Biomimetic regeneration of elastin matrices using hyaluronan and copper ion cues. Tissue Eng Part A **15,** 103, 2009.
69. Kothapalli, C.R., and Ramamurthi, A. Copper nanoparticle cues for biomimetic cellular assembly of crosslinked elastin fibers. Acta Biomater **5,** 541, 2009.
70. Kothapalli, C.R., and Ramamurthi, A. Lysyl oxidase enhances elastin synthesis and matrix formation by vascular smooth muscle cells. J Tissue Eng Regen Med **3,** 655, 2009.
71. Lin, S., Sandig, M., and Mequanint, K. Three-dimensional topography of synthetic scaffolds induces elastin synthesis by human coronary artery smooth muscle cells. Tissue Eng Part A **17,** 1561, 2011.

72. Lin, S., and Mequanint, K. The role of Ras-ERK-IL-1β signaling pathway in upregulation of elastin expression by human coronary artery smooth muscle cells cultured in 3D scaffolds. Biomaterials **33,** 7047, 2012.
73. Venkataraman, L., and Ramamurthi, A. Induced elastic matrix deposition within three-dimensional collagen scaffolds. Tissue Eng Part A **17,** 2879, 2011.
74. Venkataraman, L., Bashur, C.A., and Ramamurthi, A. Impact of cyclic stretch on induced elastogenesis within collagenous conduits. Tissue Eng Part A **20,** 1403, 2014.
75. Mourão, P.A., Luz, M.R., and Borojevic, R. Sulfated glycosaminoglycans synthesized by human smooth muscle cells isolated from different organs. Biochim Biophys Acta **881,** 321, 1986.
76. Suarez, E.R., Nohara, A.S., Mataveli, F.D., de Matos, L.L., Nader, H.B., and Pinhal, M.A. Glycosaminoglycan synthesis and shedding induced by growth factors are cell and compound specific. Growth Factors **25,** 50, 2007.
77. Dey, N.B., and Lincoln, T.M. Possible involvement of Cyclic-GMP-dependent protein kinase on matrix metalloproteinase-2 expression in rat aortic smooth muscle cells. Mol Cell Biochem **368,** 27, 2012.
78. Kuo, Y.R., Wang, F.S., Jeng, S.F., Lutz, B.S., Huang, H.C., and Yang, K.D. Nitrosoglutathione improves blood perfusion and flap survival by suppressing iNOS but protecting eNOS expression in the flap vessels after ischemia/reperfusion injury. Surgery **135,** 437, 2004.
79. Egashira, K., and Takeshita, A. Nitric oxide activity at the site of coronary spasm: deficient or preserved? Circulation **96,** 1048, 1997.
80. Fukumoto, Y., Shimokawa, H., Kozai, T., Kadokami, T., Kuwata, K., Yonemitsu, Y., Kuga, T., Egashira, K., Sueishi, K., and Takeshita, A. Vasculoprotective role of inducible nitric oxide synthase at inflammatory coronary lesions induced by chronic treatment with interleukin-1beta in pigs *in vivo*. Circulation **96**, 3104, 1997.
81. Buttery, L.D., Springall, D.R., Chester, A.H., Evans, T.J., Standfield, E.N., Parums, D.V., Yacoub, M.H., and Polak, J.M. Inducible nitric oxide synthase is present within human atherosclerotic lesions and promotes the formation and activity of peroxynitrite. Lab Invest **75,** 77, 1996.

Address correspondence to:
Chandrasekhar R. Kothapalli, PhD
Department of Chemical and Biomedical Engineering
Cleveland State University
2121 Euclid Ave., FH 460
Cleveland, OH 44115

E-mail: c.kothapalli@csuohio.edu

Received: June 18, 2014
Accepted: January 7, 2015
Online Publication Date: March 6, 2015